Density Functional Theory/Time-dependent DFT Studies on the Structures, Trend in DNA-binding Affinities, and Spectral Properties of Complexes $[Ru(bpy)_2(p\text{-R-pip})]^{2+}$ (R = −OH, $-CH_3$, −H, $-NO_2$)

Jun Li,[†] Lian-Cai Xu,[†] Jin-Can Chen,[†] Kang-Cheng Zheng,*[,†] and Liang-Nian Ji*[,†,‡]

School of Chemistry and Chemical Engineering/The Key Laboratory of Gene Engineering of Ministry of Education, Sun Yat-Sen University, Guangzhou 510275, P. R. China, and Department of Chemistry, Tongji University, Shanghai 200092, P. R. China

Received: November 8, 2005; In Final Form: May 5, 2006

Studies on the electronic structures and trend in DNA-binding affinities of a series of Ru(II) complexes $[Ru(bpy)_2(p\text{-R-pip})]^{2+}$ (bpy = 2,2-bipyridine; pip = 2-phenylimidazo[4,5-*f*] [1,10]-phenanthroline; R = −OH, $-CH_3$, −H, $-NO_2$) **1**−**4** have been carried out, using the density functional theory (DFT) at the B3LYP/LanL2DZ level. The electronic absorption spectra of these complexes were also investigated using time-dependent DFT (TDDFT) at the B3LYP//LanL2DZ/6-31G level. The computational results show that the substituents on the parent ligand (pip) have a significant effect on the electronic structures of the complexes, in particular, on the energies of the lowest unoccupied molecular orbital (LUMO) and near some unoccupied molecular orbitals (LUMO+x, $x = 1-4$). With the increase in electron-withdrawing ability of the substituent in this series, the LUMO+x ($x = 0-4$) energies of the complexes are substantially reduced in order, for example, $\epsilon_{LUMO}(\mathbf{1}) \approx \epsilon_{LUMO}(\mathbf{2}) > \epsilon_{LUMO}(\mathbf{3}) > \epsilon_{LUMO}(\mathbf{4})$, whereas the π-component populations of the LUMO+x ($x = 0-4$) are not substantially different. Combining the consideration of the bigger steric hindrance of complex **2**, the trend in DNA-binding affinities (K_b) of the complexes, that is, $K_b(\mathbf{2}) < K_b(\mathbf{1}) < K_b(\mathbf{3}) < K_b(\mathbf{4})$ can be reasonably explained. In addition, the experimental singlet metal-to-ligand charge transfer (^{1}MLCT) spectra of these complexes can be well simulated and discussed by the TDDFT calculations.

1. Introduction

The interactions of Ru(II) polypyridyl-type complexes with DNA have attracted considerable attention for many years,[1−4] because of their potential utilities in DNA structure probes[1,4] DNA molecular light switches,[5−7] DNA-dependent electron transfer probes,[3] chemotherapy and photodynamic therapy,[4] and sequence-specific cleaving agents through DNA,[8−10] and so forth. The well-known $[Ru(phen)_2(dppz)]^{2+}$ and $[Ru(bpy)_2(dppz)]^{2+}$ complexes are the most extensively investigated complexes as molecular "light switches" for DNA, because such complexes exhibit a negligible background emission in water but exhibit an intense luminescence in the presence of double-stranded DNA.[6,7] Recently, a series of derivatives of $[Ru(L)_2(dppz)]^{2+}$ (L = bpy, phen) as parent complexes have been synthesized through substitution on the intercalative ligand (dppz) to improve the luminescence property of the complexes as molecular "light switches" for DNA.[11,12] However, so far, better "light switch" complexes than the above parent complexes have not been found yet. It is notable that the complex $[Ru(bpy)_2(pip)]^{2+}$ and a series of its derivatives having a comparably excellent molecular "light switch" property, for example, the complex $[Ru(bpy)_2(hnoip)]^{2+}$, and so forth, have been reported.[13−15]

The excellent molecular "light switch" properties of complexes must relate closely to their electronic structures, since each octahedral polypyridyl Ru(II) complex is formed from a central metal ion and three polypyridyl ligands with conjugated π-bonds and there are two N atoms as coordination points in each ligand. Since the conjugated π-bonds of the three ligands all go through the center atom Ru(II), the π-electrons can move throughout the whole molecule, and thus the complex is a very large conjugated system. Changing the substitutive group or substituent position on the intercalative ligands can make some interesting differences in the DNA-binding affinities and related properties of the Ru(II) polypyridyl complexes.[16−18] Therefore, Ru(II) polypyridyl complexes have also attracted much attention from theoretical chemists, and many theoretical researchers have tried to correlate the experimental findings with theoretical predictions. In particular, more and more computations applying the DFT method[19−22] to this field have been reported,[23−29] because DFT calculations consider electron correlation energies very well, obviously reducing the computational expenses.[22,24] These theoretical efforts on the electronic structures and related properties of the complexes are very significant in guiding the analysis of the DNA-binding mechanism as well as the functional molecular design of this kind of Ru(II) complex.[25−29]

On the other hand, time-dependent density functional theory (TDDFT), found in 1984 by Runge and Gross,[30] can be viewed as an exact reformulation of the time-dependent quantum mechanics, and it recently has become one of the most popular methods for the calculations of electronic spectra and excited states of medium-sized and large molecules (up to 200 second-row atoms),[31−33] although TDDFT introduces errors by using approximate exchange-correlation (xc) functionals and is being improved for long-range charge-transfer excited states.[34,35]

* To whom correspondence should be addressed. E-mail: ceszkc@sysu.edu.cn (K.-C.Z.); cesjln@sysu.edu.cn (L.-N.J.).
† Sun Yat-Sen University.
‡ Tongji University.

10.1021/jp0564389 CCC: $33.50
Published on Web 06/14/2006

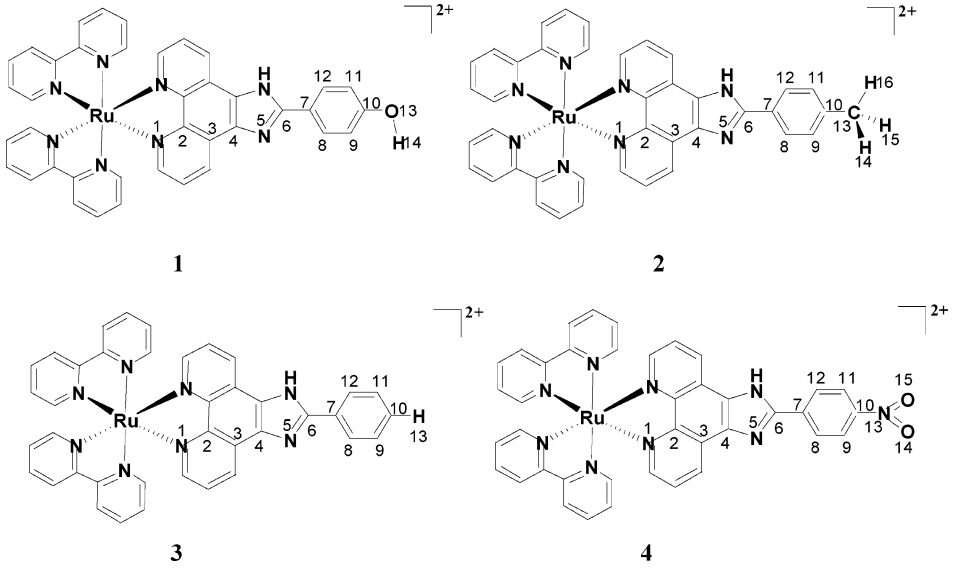

Figure 1. Structural schematic diagrams of $[Ru(bpy)_2(p\text{-R-pip})]^{2+}$ (R = −OH, $-CH_3$, −H, $-NO_2$) **1**−**4**.

TABLE 1: Computational Selected Bond Lengths (nanometers), Bond Angles (deg), and Dihedral Angles (deg) of Complexes Using the DFT at the B3LYP/LanL2DZ Level

							dihedral angle		
comp.	$Ru-N_m$[a]	$Ru-N_{co}$	$C-C(N)_m$[b]	$C-C(N)_{co}$	A_m[c]	A_{co}	C9−C10−X13−Y14[d]	N5−C6−C7−C8	N5−C6−C7−C12
0 (calc)	0.2101	0.2101	0.1400	0.1400	78.4	78.4			
$[Ru(bpy)_3]^{2+}$(expt)	0.2056	0.2056	0.1369	0.1369	78.7	78.7			
1 (R = −OH)	0.2108	0.2097	0.1405	0.1400	79.3	78.5	−0.02	0.54	−179.40
2 ($R = -CH_3$)	0.2108	0.2097	0.1406	0.1400	79.3	78.5	59.58	0.82	−179.13
3 (R = −H)	0.2108	0.2097	0.1406	0.1400	79.3	78.5		0.79	−179.17
4 ($R = -NO_2$)	0.2107	0.2098	0.1405	0.1400	79.2	78.5	0.01	0.43	−179.53

[a] $Ru-N_m$ expresses the mean coordination bond length between Ru and N atoms of the main ligand L(*p*-R-pip) (R = −OH, $-CH_3$, −H, $-NO_2$), and $Ru-N_{co}$ expresses that between Ru and N atoms of the coligand (bpy). [b] $C-C(N)_m$ expresses the mean bond length of the ring skeleton of the main ligand. [c] A_m expresses the coordination bond angle between Ru and two N atoms of the main ligand. [d] In C9−C10−X13−Y14: X = O,Y = H for **1**; X = C, Y = H for **2**; and X = N, Y = O for **4**.

Recently, TDDFT has been successfully used to calculate the electronic spectra of transition metal complexes such as metal fluorides,[36] metal carbonyls,[37] nitrosyl complexes,[38] quinone−catechol complexes,[39] and metalloporphyrins.[40] More recently, an extensive series of TDDFT calculations on several ligands and related Ru(II) complexes have been reported.[29,41−45]

In this paper, the theoretical studies on the promising "light switch" complex $[Ru(bpy)_2(pip)]^{2+}$ and its substitutive derivatives $[Ru(bpy)_2(p\text{-R-pip})]^{2+}$ (R = −OH, $-CH_3$, $-NO_2$) applying the DFT method were carried out. The effects of some substituents on the intercalative ligands on the geometric and electronic structures of the complexes were investigated. This paper is mainly focused on theoretically exploring the trend in DNA-binding affinities of this series of complexes. In addition, the singlet metal-to-ligand charge transfer (^{1}MLCT) spectra of the complexes were also computed, simulated, and discussed by the TDDFT method.

2. Computational Methods

Structural schematic diagrams of the octahedral complexes $[Ru(bpy)_2(p\text{-R-pip})]^{2+}$ (R = −OH, $-CH_3$, −H, $-NO_2$) **1**−**4** are shown in Figure 1. Every one of the four complexes is formed from one Ru(II) atom, one main ligand L (*p*-R-pip) or called the intercalative ligand, and two coligands (bpy). There is no symmetry in these complexes. Seventy-six to seventy-nine atoms are involved in each complex. The DFT-B3LYP method[19−22] and the LanL2DZ basis set (ECP+DZ for the Ru atom, D95 for the other atoms)[22,46,47] were adopted. The full geometry optimization computations were carried out for the ground states of these complexes with the singlet state.[48] Furthermore, the stable configurations of these complexes can be confirmed by frequency analysis, in which no imaginary frequency was found for all configurations at the energy minima. To perform accurately the UV−vis spectral computations by using the time-dependent DFT (TDDFT), the B3LYP approach and LanL2DZ/6-31G basis set (ECP +DZ for the Ru atom and 6-31G for the other atoms (C, N, O, and H atoms)) were adopted. Forty singlet-excited-state energies of the complexes in vacuo were calculated. In addition, to vividly depict the detail of the frontier molecular orbitals, the stereocontour graphs of some related frontier molecular orbitals of the complexes for the ground states were drawn with the Molden v3.7 program[49] based on the computational results. All calculations were performed with the Gaussian 98 quantum chemistry program package (revision A.11.4).[50]

3. Results and Discussion

3.1. Substituent Effects on Selected Bond Lengths and Bond Angles of the Complexes. The computational results and experimental data for the selected bond lengths and bond angles of the complexes are shown in Table 1. First, the coordination bond length (0.2101−0.2108 nm) of the main ligand for every one of the $[Ru(bpy)_2(p\text{-R-pip})]^{2+}$ (R = −OH, $-CH_3$, −H, $-NO_2$) is slightly longer than that (0.2097−0.2101 nm) of the coligand. Second, the mean bond length of the ligand skeleton for every complex is very close to its standard bond length

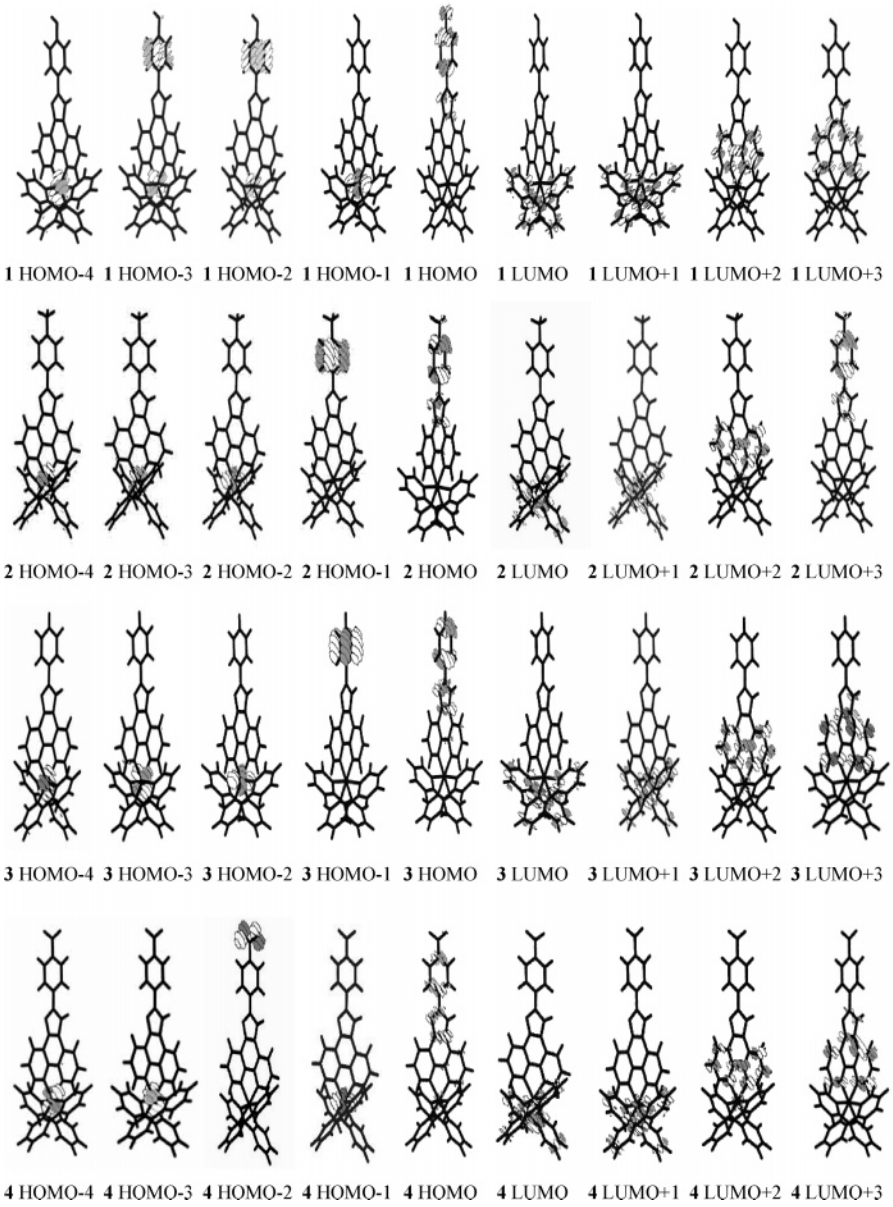

Figure 2. Some related frontier MO contour plots of complexes $[Ru(bpy)_2(p\text{-R-pip})]^{2+}$ (R = −OH, $-CH_3$, −H, $-NO_2$) **1**−**4** using the DFT method at the B3LYP/LanL2DZ level.

(0.140 nm)[51] and that of the main-ligand skeleton is also slightly longer than that of the coligand. Third, there is not a substantial difference in the calculated geometric data of the complexes except for the dihedral angles (reflecting planarity) of their main ligands. All dihedral angles of the main ligands for complexes **1**, **3**, and **4** are close to 0.00°, or ±180.00°, such facts prove that their main ligands all possess a good planarity and thus a small steric hindrance for their parallel intercalating between the adjacent π-planes of base pairs of DNA. However, for complex **2**, the dihedral angles C9−C10−C13−H14 are 59.58°, such a fact suggests that the main ligand of complex **2** has a relatively poor planarity and that the steric hindrance of its main ligand is relatively big (because of $-CH_3$).

Comparing the computed results of the parent complex $[Ru(bpy)_3]^{2+}$ (**0**)[48,52] with its experimental data (see in Table 1), we can find that the computed bond lengths are generally longer than the corresponding experimental data slightly, for example, the computed coordination bond lengths (Ru−N) are greater than the experimental ones by ∼2%. Although the direct comparisons between the computed results and the corresponding experimental values for the studied four complexes are not performed because the reports on their crystal structures have not been found yet, the results of the full geometry optimization computations by the DFT method should be reliable according to the comparison between the calculated results and experimental data of the parent complex $[Ru(bpy)_3]^{2+}$. The above calculated errors from the experimental data can be thought of as systemic errors caused by the computational method and environmental factors. Therefore, on the basis of the computed geometries of the complexes, we can further carry out the studies on the electronic structures and the trend in DNA-binding affinities and related properties of complexes $[Ru(bpy)_2(p\text{-R-pip})]^{2+}$ (R = −OH, $-CH_3$, −H, $-NO_2$).

3.2. Characteristics of the Electronic Structures of the Complexes. 3.2.1. Frontier Molecular Orbital Components. The frontier molecular orbitals, in particular, the highest occupied molecular orbital (HOMO) and the lowest unoccupied molecular orbital (LUMO) are very important because they relate not only to the spectral properties but also to the trend in DNA-binding affinities of the complexes. The stereocontour graphs of the some frontier molecular orbitals of the complexes are shown in Figure 2.

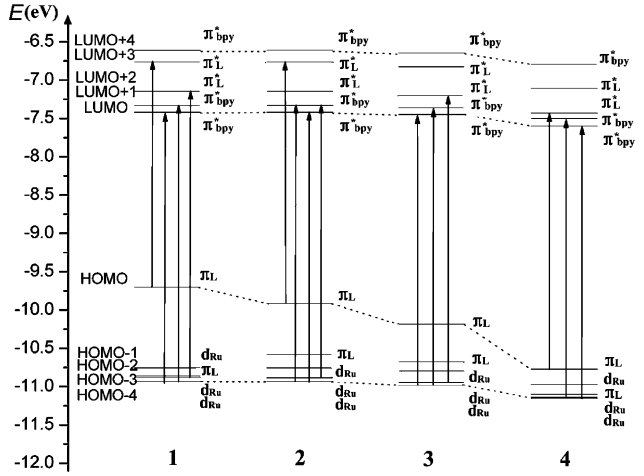

Figure 3. Energy levels of some frontier molecular orbitals of $[Ru(bpy)_2(p\text{-R-pip})]^{2+}$ (R = −OH, $-CH_3$, −H, $-NO_2$) **1**−**4** using the DFT at the B3LYP/LanL2DZ level (arrowheads express some transitions, most contributing to the experimental ^{1}MLCT band (400−500 nm) with the TDDFT method; see Table 3).

TABLE 2: Absorption Spectra (λ_{max}) and DNA-binding Constants (K_b) of $[Ru(bpy)_2(p\text{-R-pip})]^{2+}$ (R = −OH, $-CH_3$, −H, $-NO_2$) 1−4 as Well as Related References

complex	λ_{max} (nm)	K_b (M^{-1})	ref
1	458	$(0.7-1.0) \times 10^5$	53
2	458	2.0×10^4	54
3	458	4.7×10^5	55
4	460	$(7.2-7.6) \times 10^5$	56

From Figure 2, we can see that there are some common characteristics in the components of some frontier molecular orbitals of the four complexes $[Ru(bpy)_2(p\text{-R-pip})]^{2+}$ (R = −OH, $-CH_3$, −H, $-NO_2$) **1**−**4**. All the components of the HOMO−3 and HOMO−4 of complexes **1**−**4** come mainly from the d orbitals of the center metal atom (Ru), and they can be characterized by the d orbitals of the metal atom. Furthermore, the components of the LUMO and LUMO+x (x = 1−4) of the four complexes are all very close, that is, their components of the LUMO and LUMO+1 come mainly from the p orbitals of the C and N atoms of the coligand (bpy) whereas those of the LUMO+2 and LUMO+3 come mainly from the p orbitals of the C and N atoms of the main ligand (L). The component characteristics of the frontier molecular orbitals of these complexes will be helpful in understanding their trend in DNA-binding affinities and spectral properties.

3.2.2. Frontier Molecular Orbital Energies. The computed energies of some frontier molecular orbitals (MOs) using the DFT method at the B3LYP/LanL2DZ level are shown in Figure 3. These energies are all negative and rather low, and thus it shows that these complexes are very excellent electron acceptors in their DNA binding. Moreover, the LUMO energies (ϵ_{LUMO}) of these complexes are −7.420, −7.417, −7.450, and −7.600 eV, respectively, that is, ϵ_{LUMO}(**1**) ≈ ϵ_{LUMO}(**2**) > ϵ_{LUMO}(**3**) > ϵ_{LUMO}(**4**), and the orders of their LUMO+x (x = 1−4) energies are all similar to that of their LUMO energies (ϵ_{LUMO}).

3.3. Theoretical Explanation of the Trend in DNA-binding Affinities of the Complexes. To compare quantitatively the DNA-binding affinities of these complexes, the intrinsic binding constants K_b of the complexes to calf thymus (CT) DNA have been measured experimentally with spectroscopic methods,[53−56] as shown in Table 2. Obviously, the trend in DNA-binding constants (K_b) of this series of complexes is K_b(**2**) < K_b(**1**) < K_b(**3**) < K_b(**4**). Such a trend can be reasonably explained by the DFT calculations.

As is well-established, there are $\pi-\pi$ stacking interactions in the DNA-binding of Ru(II) polypyridyl-type complexes in an intercalation (or part intercalation) mode.[5,57] Furthermore, many of the theoretical studies have shown that a DNA molecule is an electron donor and an intercalated complex is an electron acceptor.[24,58] For example, on the basis of DFT calculations and the frontier molecular orbital theory,[59,60] Reha and Hobza et al. reported that all isolated intercalators (ethidium, daunomycin, ellipticine, and 4′,6-diaminide-2-phenylindole) binding to DNA are good electron acceptors because their LUMO energies are almost negative, whereas all isolated bases and base pairs of DNA (e.g., adenine, thymine, and adenine−thymine) are very poor electron acceptors because their LUMO energies are all positive.[58] Kurita and Kobayashi further reported a better simplified approximation model for DNA (stacked DNA base pairs with backbones) and its DFT-computed results.[24] They should be useful and feasible for our discussion. The energies of the HOMO and seven occupied MOs lying near to the HOMO for the CG/CG stacking calculated by the authors were −1.27, −1.33, −1.69, −1.79, −1.98, −2.06, and −2.08 eV, respectively. Their results indicate that the HOMO energy and the energies of some occupied orbitals near to the HOMO are rather high and that the HOMO and HOMO−1 are predominately distributed on the base pairs of DNA, and thus, such results offer a further theoretical foundation for the bases and base pairs being good electron donors. We have performed the calculations for the four Ru(II) complexes using the DFT method, and the calculated energies of their LUMOs and four unoccupied MOs lying near to the LUMOs (LUMO+x, x = 1−4) are not only negative but also rather low, within the range of −7.60 to −6.61 eV. These energies are much lower than the above energies of the frontier occupied MOs of the stacked DNA base pairs with backbones, and the components of these MOs are predominantly distributed on ligands, in particular, on intercalative ligands (see Figure 2). When one ligand (L) parallelly intercalates between two adjacent π-planes of DNA base pairs, the LUMO of the complex must easily accept the electrons (or "electron cloud") from the HOMO of the DNA base pairs based on the frontier molecular orbital theory. Recently, we have also reported some DFT results on the electronic structures and the trend in DNA-binding affinities of complexes $[Ru(bpy)_2L]^{2+}$ (L = *o*-hpip, *m*-hpip, and *p*-hpip),[53] $[RuL_2(pmip)]^{2+}$ (L = bpy, phen, dmp),[54] and $[Ru(phen)_2(p\text{-L})]^{2+}$ (L = mopip, hpip, and npip)[61] and also supported the above proposals.

Therefore, the factors affecting DNA-binding affinities of the complexes can be usually considered from the planarity and plane area of an intercalative ligand and the energy and population of the lowest unoccupied molecular orbital (LUMO, even and LUMO+x) of the complex molecule.[53−58,60−62]

First, from the geometric parameters of these complexes (see Table 1), although the planarity and conjugative planar area of main-ligand skeletons of complexes **1**−**4** are not substantially different, the steric hindrance of complex **2** to its main ligand intercalating between DNA base pairs should be bigger than those of complexes **1**, **3**, and **4** because its two H atoms of $-CH_3$ are located above and below the main-ligand skeleton plane, respectively. Second, from the populations of the LUMO+x (x = 0−4) of these complexes (see Figure 2), there is not a substantial difference among them. Third, from the energies of the LUMO+x (x: 0−4) of these complexes (see Figure 3), we can see that the LUMO energies (ϵ_{LUMO}) follow the sequence of ϵ_{LUMO}(**1**) ≈ ϵ_{LUMO}(**2**) > ϵ_{LUMO}(**3**) > ϵ_{LUMO}(**4**), especially that the energies of LUMO+2, of which the components are predominantly distributed on the intercalative ligand, also follow

the sequence of $\epsilon_{LUMO+2}(\mathbf{1}) \approx \epsilon_{LUMO+2}(\mathbf{2}) > \epsilon_{LUMO+2}(\mathbf{3}) > \epsilon_{LUMO+2}(\mathbf{4})$. Since a lower LUMO energy of the complex is advantageous to accepting the electrons from DNA base pairs in an intercalative mode, if the steric hindrance of complex **2** is not considered, the trend in the DNA-binding affinities of the complexes should increase in order from complex **1** to complex **4**, that is, the increase in the electron-withdrawing ability of the substituent is advantageous to the improvement of DNA-binding affinity of the complex. Altogether, the substitution of an electron-withdrawing group for H on the intercalative ligand is advantageous to reducing the energies of the LUMO and LUMO+x and thus to improving the DNA-binding affinity of the substituted complex.

Synthetically considering the above three factors, it is easily deduced that the DNA-binding affinity of complex **4** should be the greatest, because all of these factors, that is, the planarity and planar area of the intercalative ligand and the energies of the LUMO, are all advantageous to the interaction between this complex and DNA. The next one is complex **3**, since its LUMO energy is higher than that of complex **4** but lower than those of **1** and **2**. Similarly, complex **1** follows complex **3**. As for complex **2**, its DNA-binding constant must be the smallest, because its steric hindrance effect is obviously bigger than that of complex **1**, although the LUMO energies of both complex **1** and **2** are close. Therefore, the trend in the DNA-binding constants (K_b), that is, $K_b(\mathbf{2}) < K_b(\mathbf{1}) < K_b(\mathbf{3}) < K_b(\mathbf{4})$, is reasonably explained.

3.4. Explanation on the ^{1}MLCT Spectra of the Complexes. The experimental spectra of these Ru(II) polypyridyl complexes in aqueous solution show the presence of a broad band of comparable intensity, lying in the range of 400−500 nm (as shown in Figure 4[13,53,54,56]), and such a broad band is generally assigned to a singlet metal-to-ligand charge transfer (^{1}MLCT) in the UV−vis region, and thus, it is very widely applied in bioinorganic chemistry.[48,63,64]

The electronic absorption spectra of the complexes in the UV−vis region have been computed and the features of ^{1}MLCT bands will be emphatically discussed, using the TDDFT method at the B3LYP/LanL2DZ (for Ru) and 6-31G (for other atoms) levels. The computed absorption-spectral wavelengths and their comparisons with the corresponding experimental data,[53−56] as well as the related transitions and assignments, are also given in Table 3, considering those theoretical transitions within 400−500 nm characterized by an oscillator strength (*f*) larger than 0.08 and orbital contributions larger than 10%. The simulated spectra in the range of 350−550 nm using the TDDFT method in vacuo and the corresponding experimental absorption spectra[13,53,54,56] of complexes **1**−**4** are given in Figure 4.

From Table 3, we find that, for complex **1**, three strong transitions with $f > 0.10$ lie in the range 400−500 nm. Among them, two strong transitions, that is, one at 431 nm ($f = 0.110$) and another one at 417 nm ($f = 0.145$), have obvious ^{1}MLCT character and mainly originate from HOMO−4 → LUMO (75.4%) ($d_{Ru} \rightarrow \pi^*_{bpy}$) and HOMO−3 → LUMO+1 (20.3%) ($d_{Ru} \rightarrow \pi^*_{bpy}$) for the former as well as HOMO−4 → LUMO+1 (61.7%) ($d_{Ru} \rightarrow \pi^*_{bpy}$) and HOMO−3 → LUMO+2 (22.0%) ($d_{Ru} \rightarrow \pi^*_{L}$) for the latter. However, it is notable that besides these two strong ^{1}MLCT transitions there is also a strong transition at 473 nm ($f = 0.141$) with ^{1}LL (ligand-to-ligand) character, and it mainly originates from HOMO → LUMO+3 (100.0%) ($\pi_L \rightarrow \pi^*_L$). Therefore, the experimental broad band of comparable intensity (458 nm) of complex **1**, lying in the range of 400−500 nm, should be mainly assigned to the result of superposition of the above three strong bands and assigned

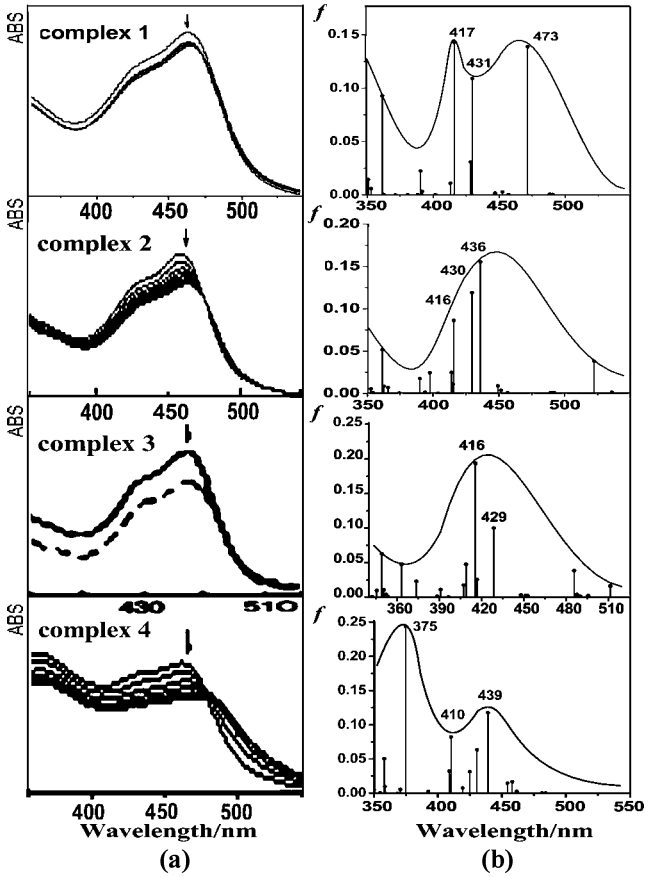

Figure 4. (a) Absorption spectra of complexes **1**−**4**.[13,53,54,56] For complex **1**: in 5 mM Tris−HCl buffer (pH 7.2), 50 mM NaCl in the presence of increasing amounts of calf thymus DNA, [DNA] = 0−3.0 × 10^{-4} mol·dm^{-3}, [Ru] = 6.0 × 10^{-6} M, and similar conditions are used for complexes **2**−**4**. The arrowhead shows the absorbance changes upon increasing amounts of CT-DNA concentration starting from [DNA] of zero.[53(ESI)] (b) Corresponding simulated spectra in 350−550 nm and oscillator strengths (*f*) using the TDDFT method in vacuo.

to the ^{1}MLCT band with a certain ^{1}LL character. In fact, a careful analysis of Figure 4 suggests there are two considerable bands in this wavelength range, that is, 458 nm (relatively high and narrow) and 425 nm (relatively low and broad). Therefore, our theoretical results suggest that the experimental band at 458 nm may mainly correspond to the theoretical transition at 473 nm, and the band at 425 nm (evaluated data, based on Figure 4) can mainly correspond to the superposition of theoretical transitions at 431 and 417 nm. On the other hand, from the contour plots of complex **1** (Figure 2) and the energy level graph (Figure 3), it is possible that the theoretical transition at 473 nm with ^{1}LL character exists because the components of the HOMO of complex **1** are mainly distributed on the main ligand and are able to overlap very well with those of its LUMO+3 (mainly distributed on the main ligand too) as well as the HOMO energy is the highest in these four complexes and thus the most active. Therefore, an experimental broad band at 458 nm with a shoulder peak at 425 nm of complex **1** can be assigned to the ^{1}MLCT band with a certain ^{1}LL character.

Similar analysis can be applied to complexes **2**−**4**. However, different from complex **1**, the experimentally corresponding two simulated bands in the range of 400−500 nm are not obviously separated and thus show a broad band at 458 (for **2** and **3**) and 460 nm (for **4**), which can be also seen in Figure 4. Therefore, such experimental broad bands can also be assigned to the ^{1}MLCT band with a certain or a little ^{1}LL character. Their special transitions and assignments are given in Table 3. It also

TABLE 3: Comparison between Computational and Experimental[13,53,54,56] Wavelengths (nanometers) of ^{1}MLCT Absorption Spectra of $[Ru(bpy)_2(p\text{-R-pip})]^{2+}$ (R = −OH, $-CH_3$, −H, $-NO_2$) 1−4 as Well as Their Assignments Using the TDDFT at the B3LYP//LanL2DZ/6-31G

	wavelength (nm)			
no.	expt	calc	f [a]	assignment
1	458	473	0.141	HOMO → LUMO+3 (100.0%)[b] $\pi_L \rightarrow \pi^*_L$
	425[c]	431	0.110	HOMO−4 → LUMO (75.4%) $d_{Ru} \rightarrow \pi^*_{bpy}$; HOMO−3 → LUMO+1 (20.3%) $d_{Ru} \rightarrow \pi^*_{bpy}$
		417	0.145	HOMO−4 → LUMO+1 (61.7%) $d_{Ru} \rightarrow \pi^*_{bpy}$; HOMO−3 → LUMO+2 (22.0%) $d_{Ru} \rightarrow \pi^*_L$
2	458	436	0.159	HOMO → LUMO+3 (92.7%) $\pi_L \rightarrow \pi^*_L$
		430	0.121	HOMO−4 → LUMO (71.7%) $d_{Ru} \rightarrow \pi^*_{bpy}$; HOMO−3 → LUMO+1 (25.8%) $d_{Ru} \rightarrow \pi^*_{bpy}$
		416	0.088	HOMO−4 → LUMO+1 (43.7%) $d_{Ru} \rightarrow \pi^*_{bpy}$; HOMO−3 → LUMO+2 (20.5%) $d_{Ru} \rightarrow \pi^*_L$
3	458	429	0.100	HOMO−4 → LUMO (67.9%) $d_{Ru} \rightarrow \pi^*_{bpy}$; HOMO−1 → LUMO+1 (29.2%) $\pi_L \rightarrow \pi^*_{bpy}$
		416	0.194	HOMO−4 → LUMO+1 (55.3%) $d_{Ru} \rightarrow \pi^*_{bpy}$; HOMO−3 → LUMO+2 (24.2%) $d_{Ru} \rightarrow \pi^*_L$
4	460	439	0.117	HOMO → LUMO+2 (68.6%) $\pi_L \rightarrow \pi^*_L$; HOMO−3 → LUMO+1 (10.7%) $d_{Ru} \rightarrow \pi^*_{bpy}$
		410	0.080	HOMO−3 → LUMO+1 (31.8%) $d_{Ru} \rightarrow \pi^*_{bpy}$; HOMO−4 → LUMO (19.9%) $d_{Ru} \rightarrow \pi^*_{bpy}$
				HOMO−4 → LUMO+1 (17.5%) $d_{Ru} \rightarrow \pi^*_{bpy}$; HOMO−4 → LUMO+2(15.4%) $d_{Ru} \rightarrow \pi^*_L$

[a] Oscillator strength. [b] The percentage contributions to wave functions of excited states are given in parentheses. [c] Evaluated data based on Figure 4 due to not offering this value in the original reference.[53]

can be seen from Table 3 that there are greater contributions from $\pi \rightarrow \pi^*$ for complexes **1**, **2**, and **4**, relative to complex **3**. Such a fact suggests that introducing a substituent (e.g., −OH, etc.) onto the main ligand (pip) can increase the ^{1}LL character of the well-known ^{1}MLCT band of the resulting complex.

The errors of the calculated wavelengths from experiment data in this series of complexes lie within 20−30 nm. Such errors maybe originate from: (1) A solvent effect may play a role to a limited extent for the simulated electronic spectra in highly polar solvents and/or solvents with hydrogen bond.[42] Here, our limited studies did not perform this rectification. We hope to further investigate these effects in future studies, even though the solvatochromism of the Ru(II) complexes is very small.[65] However, the gas-phase calculations of this kind of Ru(II) complex are still able to substantially reproduce their experimental spectra.[41,66] (2) The precision of TDDFT (using approximate xc functionals) applied to the spectra of charge-transfer excited states of the complexes is also limited. Regarding the recent comments by Dreuw and Head-Gordon,[34,35] although TDDFT is a formally exact method, one introduces errors by using approximate xc functionals leading to problems in the description of, for instance, Rydberg states, large π-states, or charge-transfer excited states. However, for our Ru(II) polypyridyl complexes, the size is not rather large and thus the distance between the metal ion and ligands is also not rather long; this may be the reason the calculations of our systems and some other systems are substantially successful.

4.Conclusions

The DFT studies of a series of complexes $[Ru(bpy)_2(p\text{-R-pip})]^{2+}$ (R = −OH, $-CH_3$, −H, $-NO_2$) **1**−**4** show that the substituents on the intercalative ligands have important effects on the electronic structures, trend in the DNA-binding affinities, and spectral properties of the complexes. The results further show the following: (1) With the increase of electron-withdrawing ability of the substituent, the LUMO+x ($x = 0-4$) energies of the complexes are substantially reduced, that is, $\epsilon_{LUMO}(\mathbf{1}) \approx \epsilon_{LUMO}(\mathbf{2}) > \epsilon_{LUMO}(\mathbf{3}) > \epsilon_{LUMO}(\mathbf{4})$, and so forth. (2) The π-component populations of the LUMO+x ($x = 0-4$) of these complexes are not substantially different. (3) The steric-hindrance effect of complex **2** also plays an unadvantageous role in its DNA binding. Synthetically considering these factors, the trend in DNA-binding affinities (K_b) of the complexes, that is, $K_b(\mathbf{2}) < K_b(\mathbf{1}) < K_b(\mathbf{3}) < K_b(\mathbf{4})$, can be reasonably explained. In addition, the experimental ^{1}MLCT spectra of this series of complexes can be well simulated and discussed by the TDDFT calculations.

Acknowledgment. The financial supports of the National Natural Science Foundation of China, the Natural Science Foundation of Guangdong Province, and the Research Fund for the Doctoral Program of Higher Education of China are gratefully acknowledged.

References and Notes

(1) Barton, J. K. *Science* **1986**, *233*, 727.
(2) Nordén, B.; Lincoln, P.; Åkerman, B.; Tuite, E. *Met. Ions Biol. Syst.* **1996**, *33*, 177.
(3) Erkkila, K. E.; Odom, D. T.; Barton, J. K. *Chem. Rev.* **1999**, *99*, 2777.
(4) Metcalfe, C.; Thomas, J. A. *Chem. Soc. Rev.* **2003**, *32*, 215.
(5) Ji, L. N.; Liu, J. G.; Zou, X. H. *Coord. Chem. Rev.* **2001**, *216−217*, 513.
(6) Friedman, A. E.; Chambron, J. C.; Sauvage, J. P.; Turro, N. J.; Barton, J. K. *J. Am. Chem. Soc.* **1990**, *112*, 4960.
(7) Hartshorn, R. M.; Barton, J. K. *J. Am. Chem. Soc.* **1992**, *114*, 5919.
(8) Jenkins, Y.; Barton, J. K. *J. Am. Chem. Soc.* **1992**, *114*, 873.
(9) Delaney, S.; Pascaly, M.; Bhattarcharya, P.; Han, K.; Barton, J. K. *Inorg. Chem.* **2002**, *41*, 1966.
(10) Ruba, E.; Hart, J. R.; Barton, J. K. *Inorg. Chem.* **2004**, *43*, 4570.
(11) Brennaman, M. K.; Meyer, T. J.; Papanikolas, J. M. *J. Phys. Chem. A* **2004**, *108*, 9938.
(12) Olofsson, J.; Wilhelmsson, L. M.; Lincoln, P. *J. Am. Chem. Soc.* **2004**, *126*, 15458.
(13) Wu, J. Z.; Ye, B. H.; Wang, L.; Ji, L. N.; Zhou, J. Y.; Li, R. H.; Zhou, Z. Y. *J. Chem. Soc. Dalton Trans.* **1997**, 1395.
(14) Xiong, Y.; He, X. F.; Zou, X. H.; Wu, J. Z.; Chen, X. M.; Ji, L. N.; Li, R. H.; Zhou, J. Y.; Yu, K. B. *J. Chem. Soc., Dalton Trans.* **1999**, 19.
(15) Liu, J. G.; Ye, B. H.; Chao, H.; Zhen, Q. X.; Ji, L. N. *Chem. Lett.* **1999**, 1085.
(16) Xiong, Y.; Ji, L. N. *Coord. Chem. Rev.* **1999**, *185−186*, 711.
(17) Tan, L. F.; Chao, H.; Li, H.; Liu, Y. J.; Sun, B.; Wei, W.; Ji, L. N. *J. Inorg. Biochem.* **2005**, *99*, 513.
(18) Collin, J. P.; Jouvenot, D.; Koizumi, M.; Sauvage, J. P. *Inorg. Chem.* **2005**, *13*, 4693.
(19) Hohenberg, P.; Kohn, W. *Phys. Rev. B* **1964**, *136*, 864.
(20) Becke, A. D. *J. Chem. Phys.* **1993**, *98*, 1372.
(21) Gorling, A. *Phys. Rev. A* **1996**, *54*, 3912.
(22) Foresman, J. B.; Frisch, M. J. *Exploring Chemistry with Electronic Structure Methods*, 2nd ed.; Gaussian Inc.: Pittsburgh, PA, 1996.
(23) Damrauer, N. H.; Weldon, B. T.; McCusker, J. K. *J. Phys. Chem. A* **1998**, *102*, 3382.
(24) Kurita, N.; Kobayashi, K. *Comput. Chem.* **2000**, *24*, 351.
(25) Nazeeruddin, M. K.; Zakeeruddin, S. M.; Baker, R. H.; Gorelsky, S. I.; Lever, A. B. P.; Gratzel, M. *Coord. Chem. Rev.* **2000**, *208*, 213.
(26) Zheng, K. C.; Wang, J. P.; Peng, W. L.; Liu, X. W.; Yun, F. C. *J. Phys. Chem. A* **2001**, *105*, 10899.
(27) Zheng, K. C.; Wang, J. P.; Shen, Y.; Kuang, D. B.; Yun, F. C. *J. Chem. Soc., Dalton. Trans.* **2002**, 111.
(28) Pourtois, G.; Beljonne, D.; Moucheron, C.; Schumm, S.; Kirsch-De Mesmaeker, A.; Lazzaroni, R.; Bredas, J. L. *J. Am. Chem. Soc.* **2004**, *126*, 683.
(29) Nazeeruddin, M. K.; De Angelis, F.; Fantacci, S.; Selloni, A.; Viscardi, G.; Liska, P.; Ito, S.; Takeru, B.; Gratzel, M. *J. Am. Chem. Soc.* **2005**, *127*, 16835.

(30) Runge, E.; Gross, E. K. U. *Phys. Rev. Lett*. **1984**, *52*, 997.
(31) Sundholm, D. *Chem. Phys. Lett.* **1999**, *302*, 480.
(32) Dreuw, A.; Dunietz, B. D.; Head-Gordon, M. *J. Am. Chem. Soc.* **2002**, *124*, 12070.
(33) Tsolakidis, A.; Kaxiras, E. *J. Phys. Chem. A* **2005**, *109*, 2373.
(34) Dreuw, A.; Head-Gordon, M. *J. Am. Chem. Soc.* **2004**, *126*, 4007.
(35) Dreuw, A.; Head-Gordon, M. *Chem. Rev.* **2005**, *105*, 4009.
(36) Adamo, C.; Barone, V. *Theor. Chim. Acta* **2000**, *105*, 169.
(37) Rosa, A.; Baerends, E. J.; van Gisbergen, S. J. A.; van Lenthe, E.; Groeneveld, J. A.; Snijders, J. G. *J. Am. Chem. Soc*. **1999**, *121*, 10356.
(38) da Silva, R. S.; Gorelsky, S. I.; Dodsworth, E. S.; Tfouni, E.; Lever, A. B. P. *J. Chem. Soc., Dalton Trans*. **2000**, 4078.
(39) Gorelsky, S. I.; da Silva, S. C.; Lever, A. B. P.; Franco, D. W. *Inorg. Chim. Acta* **2000**, *300*, 698.
(40) Nemykin, V. N.; Kobayashi, N. *Chem. Commun*. **2001**, 165.
(41) Gorelsky, S. I.; Lever, A. B. P. *J. Organomet. Chem*. **2001**, *635*, 187.
(42) Fantacci, S.; De Angelis, F.; Sgamellotti, A.; Re, N. *Chem. Phys. Lett*. **2004**, *396*, 43.
(43) Batista, E. R.; Martin, R. L. *J. Phys. Chem. A* **2005**, *109*, 3128.
(44) Fantacci, S.; De Angelis, F.; Sgamellotti, A.; Marrone, A.; Re, N. *J. Am. Chem. Soc.* **2005**, *127*, 14144.
(45) Liu, X. W.; Li, J.; Zheng, K. C.; Mao, Z. W.; Ji, L. N. *Inorg. Chim. Acta* **2005**, *358*, 3311.
(46) Hay, P. J.; Wadt, W. R. *J. Chem. Phys*. **1985**, *82*, 270.
(47) Wadt, W. R.; Hay, P. J. *J. Chem. Phys*. **1985**, *82*, 284.
(48) Juris, A.; Balzani, V.; Barigelletti, F.; Campagna, S.; Belser, P.; Von Zelewsky, A. *Coord. Chem. Rev*. **1988**, *84*, 85.
(49) Schaftenaar, G.; Noordik, J. H. *J. Comput.-Aided Mol. Des*. **2000**, *14*, 123.
(50) Frisch, M. J.; Trucks, G. W.; Schlegel, H. B.; Scuseria, G. E.; Robb, M. A.; Cheeseman, J. R.; Zakrzewski, V. G.; Montgomery, J. A.; Stratmann, R. E.; Burant, J. C.; Dapprich, S.; Millam, J. M.; Daniels, A. D.; Kudin, K. N.; Strain, M. C., Farkas, O.; Tomasi, J.; Barone, V.; Cossi, M.; Cammi, R.; Mennucci, B.; Pomelli, C.; Adamo, C.; Clifford, S.; Ochterski, J.; Petersson, G. A.; Ayala, P. Y.; Cui, Q.; Morokuma, K.; Rega, N.; Salvador, P.; Dannenberg, J. J.; Malick, D. K.; Rabuck, A. D.; Raghavachari, K.; Foresman, J. B.; Cioslowski, J.; Ortiz, J. V.; Baboul, A. G.; Stefanov, B. B.; Liu, G.; Liashenko, A.; Piskorz, P.; Komaromi, I.; Gomperts, R.; Martin, R. L.; Fox, D. J.; Keith, T.; Al-Laham, M. A.; Peng, C. Y.; Nanayakkara, A.; Challacombe, M.; Gill, P. M. W.; Johnson, B.; Chen, W.; Wong, M. W.; Andres, J. L.; Gonzalez, C.; Head-Gordon, M.; Replogle, E. S.; Pople, J. A. *Gaussian 98*, revision A.11.4; Gaussian, Inc.: Pittsburgh, PA, 2002.
(51) Pople, J. A.; Beveridge, D. L. *Approximate Molecular Orbital Theory*; McGraw-Hill: New York, 1970.
(52) Murphy, C. J.; Arkin, M. R.; Jenking, Y.; Ghatlia, N. D.; Bossmann, S. H.; Turro, N. J.; Barton, J. K. *Science* **1993**, *262*, 1025.
(53) Mei, W. J.; Liu, J.; Zheng, K. C.; Lin, L. J.; Chao, H.; Li, A. X.; Yun, F. C.; Ji, L. N. *J. Chem. Soc., Dalton. Trans*. **2003**, 1352.
(54) Xu, H.; Zheng, K. C.; Deng, H.; Lin, L. J.; Zhang, Q. L.; Ji, L. N. *New J. Chem*. **2003**, *27*, 1255.
(55) Zheng, K. C.; Deng, H.; Liu, X. W.; Li, H,; Chao, H.; Ji, L. N. *J. Mol. Struct. (THEOCHEM)* **2004**, *682*, 225.
(56) Shi, S.; Liu, J.; Li, J.; Zheng, K. C.; Tan, C. P.; Chen, L. M.; Ji, L. N. *J. Chem. Soc., Dalton. Trans*. **2005**, 2038.
(57) Zou, X. H.; Ye, B. H.; Li, H.; Zhang, Q. L.; Cao, H.; Liu, J. G.; Ji, L. N.; Li, X. Y. *J. Biol. Inorg. Chem*. **2001**, *6*, 143.
(58) Řeha, D.; Kabeláč, M.; Ryjáček, F.; Šponer, J.; Šponer, J. E.; Elstner, M.; Suhai, S.; Hobza, P. *J. Am. Chem. Soc*. **2002**, *124*, 3366.
(59) Fukui, K.; Yonezawa, T.; Shingu, H. *J. Chem. Phys*. **1952**, *20*, 722.
(60) Fleming, I. *Frontier Orbital and Organic Chemical Reaction*; Wiley: New York, 1976.
(61) Liu, J.; Mei, W. J.; Lin, L. J.; Zheng, K. C.; Chao, H.;Yun, F. C.; Ji, L. N. *Inorg. Chim. Acta* **2004**, *357*, 285.
(62) Deng, H.; Li, J.; Zheng, K. C.; Yang, Y.; Chao, H.; Ji, L. N. *Inorg. Chim. Acta* **2005**, *358*, 3430.
(63) Lumpkin, R. S.; Kober, E. M.; Worl, L. A.; Murtaza, Z.; Meyer, T. J. *J. Phys. Chem.* **1990**, *94*, 239.
(64) Olson, E. J. C.; Hu, D.; Hormann, A.; Jonkman, A.; Arkin, M. R.; Stemp, E. D. A.; Barton, J. K.; Barbara, P. F. *J. Am. Chem. Soc*. **1997**, *119*, 11458.
(65) Masui, H.; Dodsworth, E. S.; Lever, A. B. P. *Inorg. Chem*. **1993**, *32*, 258.
(66) Zhou, X.; Ren, A. M.; Feng, J. K. *J. Organomet. Chem*. **2005**, *690*, 338.